Privacy-Constrained Location Accuracy in Cooperative Wearable Networks in Multi-Floor Buildings

Elena Simona Lohan[1], Viktoriia Shubina[1,2]

[1]Tampere University, Tampere. Finland
[2]University 'Politehnica' of Bucharest, Bucharest, Romania

Abstract

This paper proposes a geometric dilution-of-precision approach to quantize the privacy-aware location errors in a cooperative wearable network with opportunistic positioning. The main hypothesis is that, a wearable inside a multi-floor building could localize itself based on cooperative pseudoranges measurements from nearby wearables, as long as the nearby wearables are heard above the sensitivity limit and as long as nearby wearables choose to disclose their own positions. A certain percentage of wearables, denoted by γ, is assumed to not want to disclose their positions in order to preserve their privacy. Our paper investigates the accuracy limits under the privacy constraints with variable γ and according to various building maps and received signal strength measurements extracted from real buildings. The data (wearable positions and corresponding power maps) are synthetically generated using a floor-and-wall path-loss model with statistical parameters extracted from real-field measurements. It is found that the network is tolerant to about 30% of the wearables not disclosing their position (i.e., opting for a full location-privacy mode).

Keywords

wearables, indoor localization, location privacy, Geometric Dilution of Precision (GDOP)

1. Introduction

According to the survey by Grand View Research, Inc. in [1], the size of the worldwide wearable technology market is anticipated to reach USD 186.14 billion by the year 2030, expanding at a compound annual growth rate (CAGR) of 14.9% over the forecast period. The rapid development of technology, including wireless technology for location tracking and health monitoring, is predicted to drive industry expansion over the next several years. As of now, wearables are using smartphones as gateways to delegate heavy computations, however, in the near future, the trend is set to change and wearable technology could have enough computational capacity to become standalone [2].

Given the widespread adoption of wearable devices and smartphones (serving as a gateway for their data processing) [3], one of the most on-demand functionalities nowadays is the ability to locate oneself within defined indoor or outdoor space [4]. When localization engines are

WIPHAL 2023: Work-in-Progress in Hardware and Software for Location Computation, June 06–08, 2023, Castellon, Spain

elena-simona.lohan@tuni.fi (E. S. Lohan); viktoriia.shubina@tuni.fi (V. Shubina)
0000-0003-1718-6924 (E. S. Lohan); 0000-0001-8178-5652 (V. Shubina)

used on power-constrained devices such as wearables, it is becoming more and more important to be able to use the signals coming from opportunistic networks to perform localization in the absence of a Global Navigation Satellite System (GNSS) chipset or in order to decrease the energy consumption at the wearable side. Indeed, opportunistic ad-hoc networks have been highly studied in order to provide seamless connectivity in situations where an infrastructure mode is not continuously available [5, 6, 7]. When various wearables found inside a certain area, such as an indoor mall or a commuting hall, are interacting with each other and do various measurements based on the received wireless signals, the exchange of information can be done in a faster and lower energy-consuming way than in an infrastructure mode. One of the convenient aspects of an opportunistic network is the possibility of a low-energy cooperative localization through basic information exchanges between wearables, such as pseudorange computations based on Received Signal Strengths (RSS), timing measurements, angle, or acoustic measurements [8, 9, 10]. Hence, not only high-end wearables but also low-cost wearables could perform cooperative self-positioning through these basic information exchanges. One of the drawbacks of such opportunistic positioning with wearables is the inherent risk in terms of user privacy, e.g., when the data exchange contains accurate location information of one's wearables. For example, for an opportunistic positioning scenario, wearable devices equipped with GNSS modules and/or Inertial Measurement Units (IMUs) acting as Anchor Nodes (ANs) for their nearby wearables with lower computational resources will have to disclose their locations to nearby nodes in order to also enable the nodes in the ANs' vicinity to self-locate (e.g., when such nearby nodes are not equipped with GNSS/IMUs). Another scenario is when all wearables in the system have only WiFi/BLE chipset, but no GNSS or IMUs, and thus the process could run iteratively, where each node takes turns to act as a mobile AN for other nodes in its vicinity, based on its previously computed position. Localization can be performed by relying on distance measurements to neighboring wearables, acting as ANs and transmitting their estimated location to the devices within range [11]. Such distance measurements, at their turn, can be obtained from time, angle, or power measurements.

RSS-based measurements are susceptible to noise, signal fluctuations, and line-of-sight (LOS) vs. non-line-of-sight (NLOS) detection difficulties and other factors, as reported, for example, in [12, 13, 14, 15]. Therefore, the study in [16] investigated the RSS-based cooperative localization challenge and used Cramer–Rao lower bound (CRLB) to compare performance of the proposed method of mitigating NLOS-related errors with the conventional approaches, showing increased performance.

Another metric, acknowledged by the research community is the geometric dilution of precision (GDOP), which was originally developed to assess the precision of location estimates in GNSS [17, 6, 18, 19]. This metric fundamentally explains how the placement of the transmitters (i.e., the ANs in a terrestrial network or the satellites in GNSS) influences the precision of the estimated location and quantifies the effect of the network topology on the precision of location estimates.

However, indoor localization systems may use various technologies, such as WiFi, Bluetooth, ultrasonic, or infrared, for determining the position of a user or object within a building [20, 21]. When applying the GDOP concept to indoor localization, it is used to evaluate the geometry of the infrastructure, such as access points or beacons, that provide positioning information [22]. The more evenly distributed the infrastructure, the better the geometry and the lower the GDOP

value, which in turn results in more accurate location estimates.

Based on the literature review, one can infer that applying different metrics allows to determine circumstances when the geometry may have a detrimental impact on the localization accuracy, leading to improvements in system performance as well as its design.

The goal of this paper is to investigate the tradeoff between location accuracy on one hand (i.e., how well a wearable can locate itself based on cooperative pseudoranges measurements from nearby wearables) and the location privacy on another hand (i.e., the percentage of wearables deciding to disclose their location, with or without a perturbation, as well as the amount of intentional positioning errors or perturbations with which the nearby wearables are disclosing their location). We propose a model which includes the inherent measurement errors in a cooperative and opportunistic location-estimation algorithm, the intentional positioning errors derived for example from various obfuscation or perturbation mechanisms with which the nearby wearables in a multi-floor building are disclosing their position, as well as the percentage of the wearables fully hiding their position. Our methodology is based on a GDOP approach to quantize the privacy-constraint location errors.

Some related work has been addressed by the authors in [23, 24]; however the mathematical model provided here of the location accuracy based on maximum-likelihood pseudorange estimates is new, as well as the disjoint modeling of the measurement errors, intentional (perturbation) errors, and percentage of users hiding their positions. The GDOP concept has been previously used in the context of indoor cooperative localization, for example in [6], but no privacy constraints were included in [6].

The user location privacy typically depends on three main factors: i) measurement errors statistics, or how accurately such a location is estimated based on prior knowledge and/or information collected from the nearby nodes, ii) intentional error statistics, i.e., if and how accurately the nearby wearables disclose their location – we assume that the users have full control of how and at which level of accuracy they can share own location information with other nodes (this is computed as the percentage of users disclosing their locations), and iii) number of wearables, namely how many wearables with similar locations are there in the area; this affects the probability to mistake a wearable for another one in the area; this is also related to the probability of several wearables to belong to the same user.

Other related work to location privacy protocols and metrics [25, 26, 27, 28] or location accuracy metrics [29, 30, 31] has been overviewed in [23, 24]. As emphasized [23], the tradeoffs between location privacy and location accuracy are still insufficiently mapped out in the current literature, especially in the context of opportunistic wearable scenarios. Additional surveys on the location privacy and location accuracy tradeoffs can be found, for example, in [32, 33, 34].

The rest of the paper is organized as follows: Section 2 focuses on the system mathematical model that takes into account the privacy constraints and on the proposed GDOP-based metric. Section 3 presents the simulation environment and the simulation-based results. Section 4 summarizes the findings and discusses some future research topics in the field.

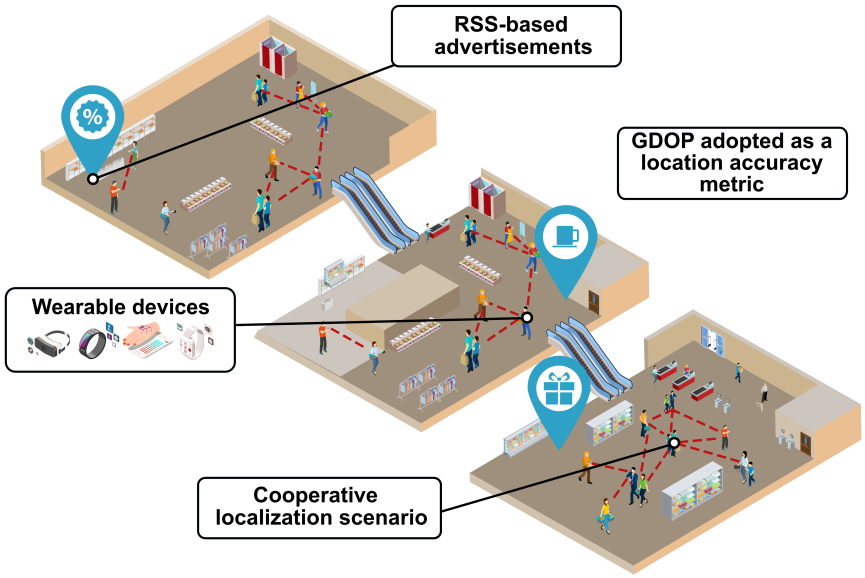

Figure 1: Illustration of an indoor multi-floor scenario used in the simulation to assess location accuracy.

2. System Model and GDOP-based accuracy metric

To illustrate the considered environment, we provide a graphical example of a potential indoor scenario for the opportunistic exchange of positioning information in Fig. 1, and in the latter part of this section, we explain the modeling parameters used in the simulations.

Fig. 1 shows a schematic floor plan of an indoor setting, such as a shopping mall. To offer the context, the users are assumed to be distributed across three floors, and this setting could be used for various location-based services, such as finding a friend, finding the nearest shop with certain items of interests, finding the nearest exit, etc. The notion of proximity detection may be utilized, for example, for counting passive encounters [35], to enhance the tourism experience [36], for sociometric applications [37], etc. It can also be used to assist individuals in navigating their surroundings. Another application of indoor positioning is the use of digital contact tracing in public places. In such a context, proximity detection could be employed to alert persons when they are too close to one another, assisting in maintaining of safe distances, and in the prevention of infection spread [38]. Indoor proximity detection can be used to track the whereabouts of valuable assets within a warehouse or factory, such as equipment, cars, or goods. This could help in the optimization of processes, theft prevention, and maximizing the effectiveness of equipment [39].

Let us assume an indoor system with N_w wearables. We also assume that each wearable can perform power, time, or angle-based measurements (or a combination of those) to identify their location in the defined indoor space. We assume also that each wearable $i = 1, \ldots, N_w$ can hear a certain amount of neighbourhood wearables, denoted with N_{h_i}. A heard wearable is a wearable from which the received power is higher than the receiver sensitivity level $P_{R_{min_i}}$ of the i-th wearable. An additional LOS condition can be imposed if the target measurements are

time-based or angle-based. NLOS wearables are also assumed to be 'heard' for power-based measurements (but not for time or angle-based measurements). A pseudorange measurement $\rho_{i,j}$ is then obtained based on the power, time, or angle measurements available at each i-th wearable from all its heard neighbours j with $j = 1, \ldots, N_{h_i}$.

The pseudorange measurement $\rho_{i,j}$ is equal to the true LOS distance between i-th and j-th wearables in the system, plus an additional measurement error, denoted here by $\epsilon_{i,j}$:

$$\rho_{i,j} = ||\mathbf{p}_i - \mathbf{p}_j|| + \epsilon_{i,j}, i = 1, \ldots, N_w; j = 1, \ldots, N_{h_i} \tag{1}$$

In eq. (1), $|| \cdot ||$ is the Euclidean norm and $\mathbf{p}_i = [x_i, y_i, z_i]$ is the position vector of the i-th wearable, having the World Geodetic System 1984 (WGS84) 3D coordinates x_i, y_i, and z_i.

In our simulator, we used the assumption that all measurement errors $\epsilon_{i,j}$ are Gaussian distributed with zero mean and σ_m standard deviation of error, i.e.,

$$\epsilon_{i,j} \sim \mathcal{N}(0, \sigma_m^2). \tag{2}$$

In a cooperative dynamic system, each wearable can update iteratively its position estimate based on the positions of the heard neighbours, assuming that a fraction $1-\gamma$ of the neighbours choose to disclose their position $\tilde{\mathbf{p}}_j$, but with a random intentional error as below:

$$\tilde{\mathbf{p}}_j = \mathbf{p}_j + \xi_j \tag{3}$$

where $\tilde{\mathbf{p}}_j$ is the position disclosed by the j-th wearable with a certain intentional error ξ_j. The intentional error is a privacy measure. In our simulator, we assumed ξ_j to be Gaussian distributed with zero mean and equal to σ_ϵ standard deviation of error for all variables, i.e.,

$$\xi_j \sim \mathcal{N}(0, \sigma_\epsilon^2). \tag{4}$$

This assumption follows the model introduced in [23].To sum up, we have two categories of wearables in our system

- A fraction γ of wearables does not disclose at all their position (this ensures what we call a fully private mode)
- A fraction $1 - \gamma$ of wearables discloses their position with an intentional positioning error $\xi_j \sim \mathcal{N}(0, \sigma_\epsilon^2)$

In addition, all position estimates are assumed to suffer of some measurement errors, modeled here via $\epsilon_{i,j} \sim \mathcal{N}(0, \sigma_m^2)$; such measurement errors are inherent in any estimation system, no matter if the position estimates were based on RSS, Angle of Arrival (AOA), Time of Arrival (TOA), or a combination of them.

If we assume a maximum likelihood cooperative position estimation, e.g. similarly with [40], the estimated updated position $\hat{\mathbf{p}}_i$ is

$$
\begin{aligned}
&\hat{\mathbf{p}}_i = \\
&arg\max_{p_i} \prod_{j=1}^{N_{h_i}} \frac{f_j}{\sqrt{(2\pi)}\sigma_{i,j}} e^{\left(-\frac{||\mathbf{p}_i - \tilde{\mathbf{p}}_j - \mu_{i,j} - \rho_{i,j}||}{2\sigma_{i,j}}\right)^2}, \\
&i = 1, \ldots, N_w; j = 1, \ldots, N_{h_i} \\
&= arg\min_{p_i} \sum_{j=1}^{M_{h_i}} \left(\frac{||\mathbf{p}_i - \tilde{\mathbf{p}}_j - \mu_{i,j} - \rho_{i,j}||}{2\sigma_{i,j}}\right)^2, \\
&i = 1, \ldots, N_w; j = 1, \ldots, M_{h_i}
\end{aligned}
\tag{5}
$$

where f_j is a $0/1$ flag associated to the privacy status of each wearable (i.e., $f_j = 1$ if the nearby wearable choose to disclose its position and $f_j = 0$ if the nearby wearable does not disclose its position) and $M_{h_i} \leq N_{h_i}$ is the number of wearables in the vicinity of i-th wearable which are heard (in terms of received power being higher than the sensitivity threshold) and choosing to disclose their position (namely, the heard wearables flagged with $f_j = 1, j = 1, \ldots, N_{h_i}$).

Eq. (5) is a non-linear optimization problem which can be solved iteratively after Taylor linearization, following, for example, the procedure in [40]:

$$
\begin{aligned}
\hat{\mathbf{p}}_i^{k+1} = \hat{\mathbf{p}}_i^k + \left(G_i^T \Sigma_i^{-1} G_i\right)^{-1} G_i^T \\
\Sigma_i^{-1}\left([\rho_{i,1} \ldots \rho_{i,M_h}]^T - ||\hat{\mathbf{p}}_i^k - \tilde{\mathbf{p}}_j^k||\right)
\end{aligned}
\tag{6}
$$

where $G_i \in \mathbb{R}^{M_{h_i} \times 3} \triangleq [G_{i,1}, \ldots, G_{i,M_{h_i}}]^T$ is the Taylor linearized matrix with rows $G_{i,j}, j = 1, M_{h_i}$ from [40] equal to

$$
G_{i,j} = \left[\frac{x_i - \tilde{x_j}}{||\mathbf{p}_i - \tilde{\mathbf{p}}_\mathbf{j}||} \; \frac{y_i - \tilde{y_j}}{||\mathbf{p}_i - \tilde{\mathbf{p}}_\mathbf{j}||} \; \frac{z_i - \tilde{z_j}}{||\mathbf{p}_i - \tilde{\mathbf{p}}_\mathbf{j}||}\right] \tag{7}
$$

and $\Sigma_i = diag(\sigma_{i,1}, \ldots, \sigma_{i,M_h}) \in \mathbb{R}^{M_{h_i} \times M_{h_i}}$ is the error covariance matrix taking into account the measurement errors $\epsilon_{i,j}$ coming from the cooperative pseudorange measurements. Above, k is the iteration index in the location estimation process, $k = 1, 2, \ldots$. The initial point of the estimation $\hat{\mathbf{p}}_i^1$ can be assumed, for example, to be the true position of the i-th wearable (e.g., the wearable is placed just at the entrance of the building and had access to accurate GNSS-based position estimates) or it can be computed as the weighted centroid of heard wearables in range which discloses their position:

$$
\hat{\mathbf{p}}_i^1 = \frac{\sum_{j=1}^{M_h} w_{i,j} f_j \tilde{\mathbf{p}}_j^1}{\sum_{j=1}^{M_h} w_{i,j} f_j} \tag{8}
$$

with $w_{i,j} = 10^(P_{R_{i,j}}/10)$, and $P_{R_{i,j}}$is the RSS (in dBm) by the i-th wearable from the j-th wearable.

If we assume that we have uncorrelated measurement errors $\epsilon_{i,j}$ of zero means and equal variances $\sigma_{i,j} \triangleq \sigma_m$, then the accuracy of the location solution from eq. (6), measured as the overall variance of the location error, is directly proportional to the trace of the square root geometry matrix $H_{GDOP,i} \triangleq \sqrt{\left(G_i^T \Sigma_i G_i\right)^{-1}}$ [40]. This means that

$$\sigma_{all}^2 = \mathbf{E}\Big(trace(H_{GDOP,i})\Big), \tag{9}$$

where $\mathbf{E}(\cdot)$ is the expectation operator taken with respect to all wearables in the building.

The matrix $H_{GDOP,i}$ is also known as the GDOP matrix. The overall location error accuracy becomes thus a function of both the measurement error standard deviation σ_m as well as of the intentional error standard deviation σ_ξ (for clarity we assumed that all wearables have the same standard deviation of the measurement and intentional errors), as G_i matrix is a function of σ_ξ. Moreover, the $H_{GDOP,i}$ can be computed either based only on LOS links from wearables which choose to disclose their position (e.g., when the pseudorange measurements in eq. (1) are based on timing or angle measurements which require LOS), or based on all heard wearables which choose to disclose their position, both LOS and NLOS (e.g., this is relevant when the pseudorange estimates are based on RSS measurements, which do not necessarily require LOS).

Therefore, the overall location accuracy per wearable i can be modeled via the above-introduced GDOP-based statistics $\sigma_{overall} \triangleq H_{GDOP,i}$ and it will be a function of the measurement error σ_m, the number of wearables $\sum_{j}^{N_h} f_j$, which choose to disclose their position with some intentional error, their intentional error standard deviation σ_ξ and, possibly, of the number of LOS links.

3. Simulation-based results

3.1. Simulator description

A Matlab-based simulator has been implemented for our studies. One building map from a three-floor shopping center was used in our models, as shown in Fig. 2. The wearables are assumed uniformly distributed across the N_{floors} floors of each building and a random walk model is assumed for each wearable. The wearables can have different heights and placements, ranging from 5 cm above the floor (e.g., foot/shoe mounted wearable) to 1.8 m above floor (e.g., head-mounted wearable). The following single-slope floor-and-wall path-loss model was assumed:

$$\begin{aligned} P_{R_{i,j}} &= P_{T_j} - 10 * n_{i,j} * log_{10}||\mathbf{p}_i - \mathbf{p}_j|| \\ &- N_{innerwalls_{i,j}} L_{innerwall} - N_{outerwalls_{i,j}} L_{outerwall} \\ &- N_{floors_{i,j}} L_{fl} + \eta_{i,j} \end{aligned} \tag{10}$$

where $P_{R_{i,j}}$ is the received signal power (in dBm) of the i-th wearable from the j-th wearable, P_{T_j} is the transmit power (in dBm) of the j-th wearable, $n_{i,j}$ is the path-loss slope coefficient

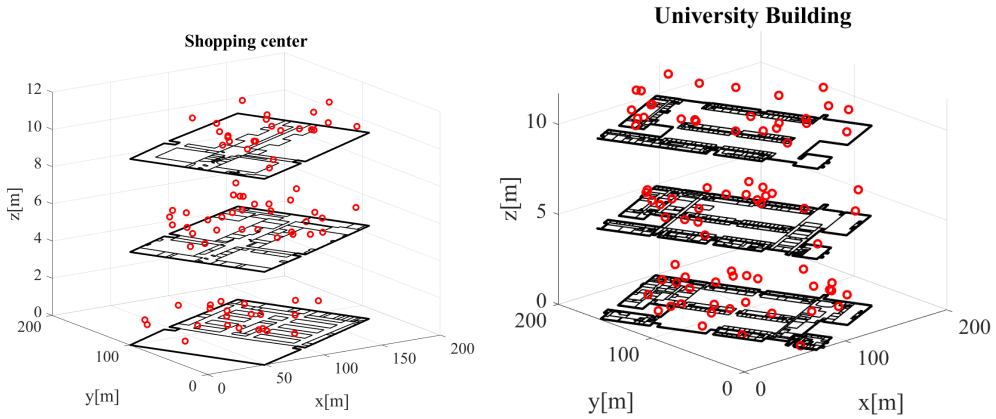

Figure 2: Illustration of the dynamic three-floor indoor simulator. The moving wearables (shown in red circles) can be used at various body heights within one floor. Left: shopping mall; right: university building

for the path connecting wearable i to wearable j (channel reciprocity condition $n_{i,j} = n_{j,i}$ was assumed to be respected), $N_{innerwalls_{i,j}}$ and $N_{outerwalls_{i,j}}$ are the numbers of inner and outer walls,respectively, between wearable i and wearable j (computed based on the building map), $N_{floors_{i,j}}$ is the number of floors between wearable i and wearable j, $L_{innerwall}$ and $L_{outerwall}$ are a loss factor (in dB) per inner or outer wall, respectively, and L_{fl} is a loss factor (in dB) per floor (all floors were assumed to introduce equal wall losses). The term $\eta_{i,j}$ models the random shadowing effects and was assumed to follow a Gaussian distribution of 0 mean and σ_{shad} standard deviation (in our simulations, $\sigma_{shad} = 4$ dB, based on the measurement results reported in [41].

A wearable j can be heard by another wearable i in the building if and only if $P_{R_{i,j}} \geq P_{R_{min_i}}$. In our simulations, the sensitivity threshold $P_{R_{min_i}}$ was set to -100dBm. Additionally, two wearables i and j are in assumed to be in LOS condition to each other if and only if $N_{walls_{i,j}} + N_{floors_{i,j}} = 0$ (and they are in a NLOS condition otherwise).

Two arbitrary examples of the synthetically generated power map from two wearables in the building is shown in Fig. 3.

A random-walk mobility model [42] with a randomly distributed velocity between 0.1 and 1 m/s was used. The wearable movements were assumed to remain at the floor of their initial position (i.e., vertical/across-floor mobility is not yet included in our model). As the building maps are proprietary, the Matlab-based simulator is not currently provided in open access.

3.2. Simulation-based results

The simulation results are based on the in-house built simulator described in Section 3.1. A total of N_w users carrying one wearable each were assumed to be distributed uniformly across the three floors of a simulated building. The buildings were based on real maps, collected from a university and from a shopping mall. The information about the building walls and floors was used in the path-loss model (see eq. (10)). All wearables are assumed to be able to hear all other wearables in the building as long as the received power is higher than the sensitivity

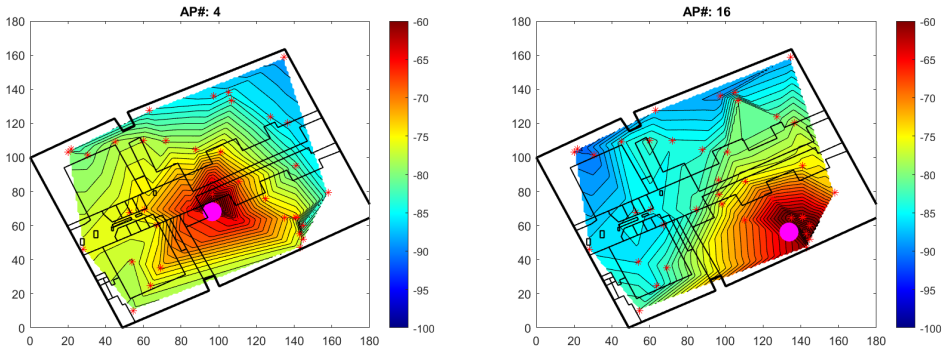

Figure 3: Illustration of the synthetically generated power map (as RSS values in dBm) for two randomly picked wearables in the building. The location of wearables acting as 'transmitters' is shown as a large magenta point, and the locations of the wearables acting as 'receivers' (i.e., where RSS values are measured) are shown in red.

threshold (in our simulations, it was set to -100 dBm). The received power values depend, of course, on the distance between any two wearables as well as on the number of walls and floors between any pair of wearables (see eq. (10)). The path-loss coefficient, inner and outer walls attenuation factors, floor attenuation factors and transmit powers of each wearable were modeled according to models extracted from real-world measurements in the two buildings based on [41], as follows

- A log-normal distribution for the transmit power P_{T_j} of each j wearable, $j = 1, \ldots, N_w$
- A normal distribution for the path loss coefficient n_j of each j wearable, $j = 1, \ldots, N_w$
- A Weibull distribution for the inner-wall $L_{innerwalls}$ and floor losses L_{fl} of each j wearable, $j = 1, \ldots, N_w$
- A Gamma distribution for the outer-wall losses $L_{outerwalls}$ of each j wearable, $j = 1, \ldots, N_w$

Fig. 4 illustrates the histograms of the path-loss parameters used in our simulations and based on field RSS measurements. Further details on choosing these parameters based on measurement data can be found in [41].

Under the assumption that a fraction γ of the wearables within a multi-floor building do not disclose their location estimates (in order to preserve their location privacy) and that all the other wearables form an opportunistic network for self-positioning, we have looked at the number of heard wearables as well as at the GDOP-based positioning accuracy in different buildings and for different γ levels. The number of heard wearables is shown in Fig. 5; the left-hand plot compares the two buildings (university building and shopping mall) assuming a small measurement noise standard deviation $\sigma_m = 0.2$ m and an intentional position error for the wearables that disclose their position of a moderate standard deviation $\sigma_\epsilon = 2$ m. The right-hand plot in Fig. 5 also shows the number of heard wearables (taken into account the path-loss propagation and γ) for three different combinations of measurement and intentional errors standard deviations $(\sigma_m, \sigma_\epsilon)$.

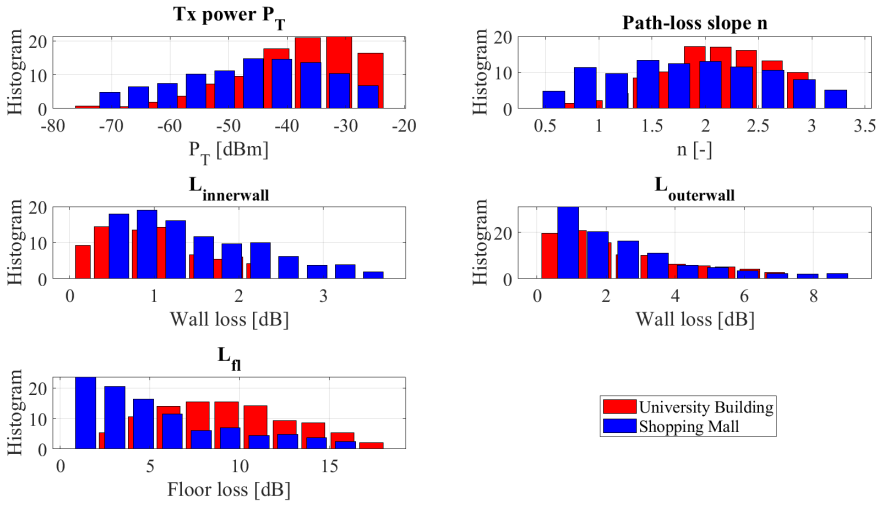

Figure 4: Distributions (histograms) of the simulation parameters in the two considered buildings.

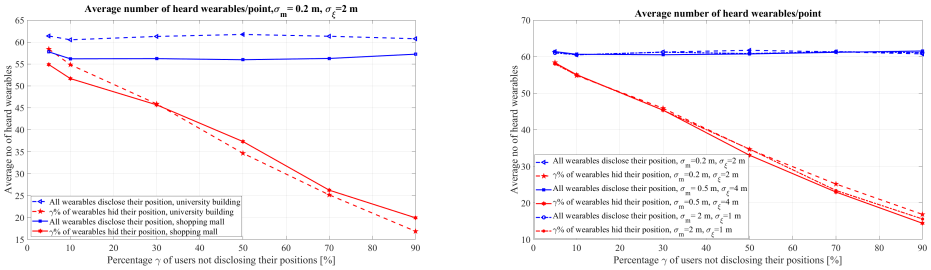

Figure 5: The average number of heard wearables versus the percentage γ of wearables not disclosing their position. 80 wearables uniformly distributed in the building and 7500 Monte Carlos runs. Left: comparison for two building maps; right: comparison for various σ_m and σ_ξ assumptions

As we can see from the left plot in Fig. 5, when all wearables disclose their position, the number of average heard number of wearables by their neighbours is a bit higher in the university building than in the shopping mall building; this can be explained if we refer to Fig. 4, where we can see that the path-loss slopes are a bit sharper and the inner wall losses are a bit higher for the shopping mall than for the university building, which means that signal attenuates faster and can go faster below the -100 dBm sensitivity limit. Surprisingly enough, when only $1-\gamma$ of the wearables disclose their position, the number of heard wearables in the two buildings are closer to each other. As expected, this number severely decreases when γ increases. The right plot in Fig. 5 focuses only on the shopping mall building and checks different combinations of $(\sigma_m, \sigma_\epsilon)$. The impact of varying $(\sigma_m, \sigma_\epsilon)$ on the number of heard wearables is very small, as expected.

The average positioning accuracy per wearable is shown in Fig. 6. Again, the left-hand plot compares the results for different buildings and the right-hand plot compares the results

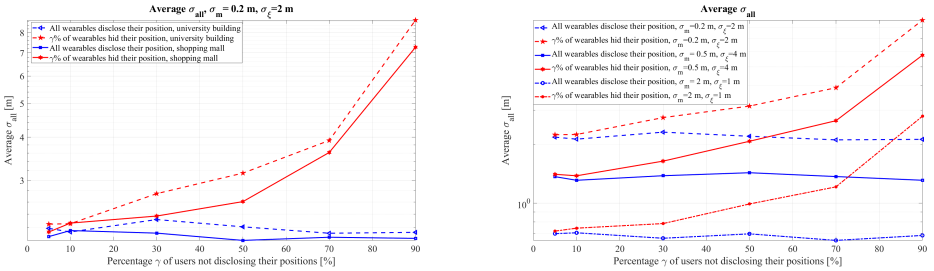

Figure 6: The average location error for all wearables in the system σ_{all} versus the percentage γ of wearables not disclosing their position. 80 wearables uniformly distributed in the building. 7500 Monte Carlos runs. Left: comparison for two building maps; right: comparison for various σ_m and σ_ξ assumptions; shopping mall building.

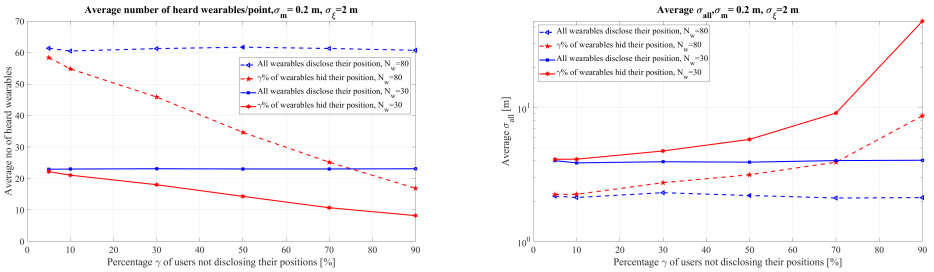

Figure 7: Impact of the number of wearables within the shopping-mall building. Left: Average number of heard wearables versus the percentage γ of wearables not disclosing their position. Right: Average location error for all wearables in the system σ_{all} versus the percentage γ of wearables not disclosing their position.

inside the shopping mall building, for different $(\sigma_m, \sigma_\epsilon)$ pairs. The blue lines are independent of γ and show the GDOP-based accuracy when all wearables disclose their position. In theory, these curves should be completely flat, but since at every Monte Carlo run we have random placement of wearables within the building and random path-loss parameters, there are small variations with 7500 Monte Carlo runs; these blue curves would converge to completely flat curves for a sufficiently high number of Monte-Carlo runs. The red lines show the deterioration in the positioning accuracy when γ increases. If we set a target of maximum 1 m accuracy deterioration, then the network would be tolerant to maximum 30% of wearables not disclosing their position (i.e., $\gamma = 0.3$ as a fraction or $\gamma = 30\%$ as a percentage; for clarity reasons, γ is given in percents in our figures). Despite the fact the the number of heard wearables was rather independent on the $(\sigma_m, \sigma_\epsilon)$, the positioning accuracy, as expected, is highly influenced by the measurement and intentional errors, as seen in the right-hand plot of Fig. 6. Again, up to $\gamma = 30\%$ offers very little degradation in the overall positioning accuracy, but for $\gamma > 30\%$, the performance starts to deteriorate fast. We would also like to emphasize the differences between the two situations: a limited number of devices all disclosing their position (let's say $N_w = 70$ devices, $\gamma = 0\%$) and the presence of some devices not willing to share their position (let's say $\gamma = 30\%$ out of $N_w = 100$ devices not sharing the position); while the overall performance will be the same in both cases (as only 70 cooperative devices that share their

positions would be available in both cases), our research question pertained to finding out how much the performance is deteriorating with respect to the maximum achievable performance (i.e., $N_w = 100$ devices in our second example) when some of them are not disclosing the position. Our findings show that such performance deterioration is not high as long as the $\gamma \leq 30\%$, no matter on the value of N_w.

Last but not least, the effect of the number of the wearables in the building is shown in Fig. 7, where we compare a situation with a low number of wearables $N_w = 30$ with a situation with a moderate number of wearables $N_w = 80$. The left-hand plots show the average number of heard wearables, which, of course, decreases when N_w decreases. The right-hand plot of Fig. 7 show again that the positioning accuracy starts to deteriorate significantly for $\gamma > 30\%$ for both $N_w = 30$ and $N_w = 80$.

To sum up, our findings show that the opportunistic network for positioning tolerates up to 30% of wearables not disclosing their position, without a significant loss in the positioning accuracy and for $\gamma > 30\%$, the accuracy starts to deteriorate significantly.

4. Conclusions and future research topics

Privacy-aware opportunistic and collaborative positioning could rely on the hypothesis that only a percentage γ of wearables within an indoor space are willing to disclose their positions. After proposing a GDOP-based positioning accuracy metric, we have investigated the robustness to such a collaborative opportunistic setup under various scenarios (building maps, number of wearables, assumptions regarding the measurement errors in estimating the position, etc.). It was shown that up to around 30% of the wearables can choose to keep their location undisclosed without a significant impact on the overall system performance.

Different random distributions of the wearables within a building as well as different mobility models of the wearables, including across-floor mobility, are to be investigated next. Furthermore, the relationship between the percentage γ of wearables hiding their position and classical location privacy metrics, such as entropy-based privacy of [23] or the normalized cell error of [24] are also to be investigated.

Acknowledgments

The authors gratefully acknowledge funding from the European Union's Horizon 2020 Research and Innovation programme under the Marie Sklodowska Curie grant agreement No. 813278 (A-WEAR, http://www.a-wear.eu/).

References

[1] Bloomberg: by Grand View Research, Inc., https://www.bloomberg.com/press-releases/2022-11-28/wearable-technology-market-to-hit-186-14-billion-by-2030-grand-view-research-inc (accessed April 2022), 2022.

[2] How AR glasses are going from niche gadget to smartphone replacement, https://www.digitaltrends.com/mobile/ar-glasses-replace-smartphones-future-how/ (accessed April 2022), 2022.

[3] H. S. Kang, M. Exworthy, Wearing the future—wearables to empower users to take greater responsibility for their health and care: Scoping review, JMIR mHealth and uHealth 10 (2022) e35684. URL: https://doi.org/10.2196/35684. doi:10.2196/35684.

[4] Y. Bello, E. Figetakis, Iot-based wearables: A comprehensive survey, arXiv preprint arXiv:2304.09861 (2023).

[5] C. B. Avoussoukpo, C. Xu, M. Tchenagnon, Ensuring Users Privacy and Mutual Authentication in Opportunistic Networks: A Survey, International Journal of Network Security 22 (2020) 118–125.

[6] B. Mukhopadhyay, S. Srirangarajan, S. Kar, Rss-based cooperative localization and edge node detection, IEEE Transactions on Vehicular Technology 71 (2022) 5387–5403. doi:10.1109/TVT.2022.3152614.

[7] G. A. Rizzo, V. Mancuso, S. Ali, M. Ajmone Marsan, Stop and forward: Opportunistic local information sharing under walking mobility, Ad Hoc Networks 78 (2018) 54–72. URL: https://www.sciencedirect.com/science/article/pii/S1570870518302403. doi:https://doi.org/10.1016/j.adhoc.2018.05.011.

[8] Y. Zhu, F. Yan, S. Zhao, S. Xing, L. Shen, On improving the cooperative localization performance for iot wsns, Ad Hoc Networks 118 (2021) 102504.

[9] O. Daniel, H. Wymeersch, J. Nurmi, Delay–accuracy tradeoff in opportunistic time-of-arrival localization, IEEE Signal Processing Letters 25 (2018) 763–767.

[10] Y. Kang, Y. Su, Y. Xu, Acgsor: Adaptive cooperation-based geographic segmented opportunistic routing for underwater acoustic sensor networks, Ad Hoc Networks 145 (2023) 103158.

[11] N. Baroutis, M. Younis, Location Privacy in Wireless Sensor Networks, Springer International Publishing, 2019, pp. 669–714. URL: https://doi.org/10.1007/978-3-319-91146-5_18. doi:10.1007/978-3-319-91146-5_18.

[12] U. M. Qureshi, Z. Umair, Y. Duan, G. P. Hancke, Analysis of bluetooth low energy (ble) based indoor localization system with multiple transmission power levels, in: 2018 IEEE 27th International Symposium on Industrial Electronics (ISIE), 2018, pp. 1302–1307. doi:10.1109/ISIE.2018.8433787.

[13] L. Flueratoru, V. Shubina, D. Niculescu, E. S. Lohan, On the high fluctuations of received signal strength measurements with ble signals for contact tracing and proximity detection, IEEE Sensors Journal 22 (2021) 5086–5100.

[14] C. Gentner, D. Günther, P. H. Kindt, Identifying the ble advertising channel for reliable distance estimation on smartphones, IEEE Access 10 (2022) 9563–9575. doi:10.1109/ACCESS.2022.3140803.

[15] X. Yang, Y. Zhuang, F. Gu, M. Shi, X. Cao, Y. Li, B. Zhou, L. Chen, Deepwipos:a deep learning-based wireless positioning framework to address fingerprint instability, IEEE Transactions on Vehicular Technology (2023) 1–16. doi:10.1109/TVT.2023.3243196.

[16] X. Tian, G. Wei, Y. Song, D. Ding, Cooperative localization based on semidefinite relaxation in wireless sensor networks under non-line-of-sight propagation, Wireless Networks 29 (2023) 775–785.

[17] S. Haigh, J. Kulon, A. Partlow, C. Gibson, Comparison of objectives in multiobjective optimization of ultrasonic positioning anchor placement, IEEE Transactions on Instrumentation and Measurement 71 (2022) 1–12. doi:10.1109/TIM.2022.3189729.

[18] M. H. Kabir, S. Lee, W. Shin, Performance evaluation of gnss positioning with geometric dilution of precision, in: 2022 13th International Conference on Information and Communication Technology Convergence (ICTC), 2022, pp. 910–912. doi:10.1109/ICTC55196.2022.9953014.

[19] Z. Deng, H. Wang, X. Zheng, L. Yin, Base station selection for hybrid TDOA/RTT/DOA positioning in mixed LOS/NLOS environment, Sensors 20 (2020) 4132. URL: https://doi.org/10.3390/s20154132. doi:10.3390/s20154132.

[20] F. U. Khan, A. N. Mian, M. T. Mushtaq, Experimental testbed evaluation of cell level indoor localization algorithm using wi-fi and lora protocols, Ad Hoc Networks 125 (2022) 102732.

[21] W. Ahmad, G. Husnain, S. Ahmed, F. Aadil, S. Lim, et al., Received signal strength-based localization for vehicle distance estimation in vehicular ad hoc networks (vanets), Journal of Sensors 2023 (2023).

[22] Z. Wu, Z. Yao, M. Lu, Optimal beacon deployment for positioning in cluttered indoor environments, IEEE Sensors Journal (2023).

[23] V. Shubina, A. Ometov, S. Andreev, D. Niculescu, E. S. Lohan, Privacy versus location accuracy in opportunistic wearable networks, in: 2020 International Conference on Localization and GNSS (ICL-GNSS), 2020, pp. 1–6.

[24] V. Shubina, A. Ometov, D. Niculescu, E. S. Lohan, Acceptable margin of error: Quantifying location privacy in ble localization, in: 2023 International Conference on Localization and GNSS (ICL-GNSS), 2023.

[25] K. Järvinen, H. Leppäkoski, E.-S. Lohan, P. Richter, T. Schneider, O. Tkachenko, Z. Yang, PILOT: Practical Privacy-Preserving Indoor Localization Using Outsourcing, in: Proc. of IEEE European Symposium on Security and Privacy (EuroS&P), IEEE, 2019, pp. 448–463.

[26] J. Z. Hare, J. Song, S. Gupta, T. A. Wettergren, POSE. R: Prediction-based Opportunistic Sensing for Resilient and Efficient Sensor Networks, arXiv preprint arXiv:1910.10795 (2019).

[27] R. Shokri, J. Freudiger, J.-P. Hubaux, A Unified Framework for Location Privacy, Technical Report, LCA, EPFL, Switzerland, 2010. URL: http://infoscience.epfl.ch/record/148708.

[28] M. Duckham, L. Kulik, A Formal Model of Obfuscation and Negotiation for Location Privacy, in: Proc. of International Conference on Pervasive Computing, Springer, 2005, pp. 152–170.

[29] N. Alsindi, B. Alavi, K. Pahlavan, Spatial characteristics of UWB TOA-based ranging in indoor multipath environments, in: Proc. of 18th International Symposium on Personal, Indoor and Mobile Radio Communications, IEEE, 2007, pp. 1–6.

[30] T. Otim, A. Bahillo, L. E. Díez, P. Lopez-Iturri, Peio and F. Falcone, Impact of Body Wearable Sensor Positions on UWB Ranging, IEEE Sensors Journal 19 (2019) 11449–11457.

[31] T. Otim, A. Bahillo, L. E. Díez, P. Lopez-Iturri, F. Falcone, FDTD and Empirical Exploration of Human Body and UWB Radiation Interaction on TOF Ranging, IEEE Antennas and Wireless Propagation Letters 18 (2019) 1119–1123.

[32] M. Zurbarán, L. González, P. W. Rojas, M. Labrador, A survey on privacy in location-based services, ingeniería y desarrollo 32 (2014) 314–343. URL: https://doi.org/10.14482/inde.32.2.

6128. doi:10.14482/inde.32.2.6128.

[33] H. Jiang, J. Li, P. Zhao, F. Zeng, Z. Xiao, A. Iyengar, Location privacy-preserving mechanisms in location-based services, ACM Computing Surveys 54 (2021) 1–36. URL: https://doi.org/10.1145/3423165. doi:10.1145/3423165.

[34] J. Zhang, J. Zhou, J. Li, J. Gu, Q. Zhang, B. Dai, Y. Wang, J. Wang, Y. Zhong, Q. Li, Location accuracy improvement of long-range lightning detection network in china by compensating ground wave propagation delay, Remote Sensing 14 (2022) 3397. URL: https://doi.org/10.3390/rs14143397. doi:10.3390/rs14143397.

[35] S. Das, S. Chatterjee, S. Chakraborty, B. Mitra, An unsupervised model for detecting passively encountering groups from wifi signals, in: 2018 IEEE Global Communications Conference (GLOBECOM), 2018, pp. 1–7. doi:10.1109/GLOCOM.2018.8647751.

[36] A. Gala, C. Borgaonkar, V. Kulkarni, M. Wakode, G. Kale, Contextual flow of information in tourism using ble proximity detection to enhance the tourism experience, in: 2023 International Conference on Emerging Smart Computing and Informatics (ESCI), 2023, pp. 1–6. doi:10.1109/ESCI56872.2023.10100063.

[37] J. Tuesta, D. Albornoz, G. Kemper, C. A. Almenara, A sociometric sensor based on proximity, movement and verbal interaction detection, in: 2019 International Conference on Information Systems and Computer Science (INCISCOS), 2019, pp. 216–221. doi:10.1109/INCISCOS49368.2019.00042.

[38] C.-E. Juneau, A.-S. Briand, P. Collazzo, U. Siebert, T. Pueyo, Effective contact tracing for covid-19: A systematic review, Global Epidemiology (2023) 100103.

[39] K. Szyc, M. Nikodem, M. Zdunek, Bluetooth low energy indoor localization for large industrial areas and limited infrastructure, Ad Hoc Networks 139 (2023) 103024.

[40] L. Heng, G. X. Gao, Accuracy of range-based cooperative positioning: A lower bound analysis, IEEE Transactions on Aerospace and Electronic Systems 53 (2017) 2304–2316.

[41] P. Richter, M. Valkama, E. S. Lohan, Attack tolerance of rss-based fingerprinting, in: 2018 IEEE Wireless Communications and Networking Conference (WCNC), 2018, pp. 1–6. doi:10.1109/WCNC.2018.8376977.

[42] H. Nurminen, M. Koivisto, S. Ali-Löytty, R. Piché, Motion model for positioning with graph-based indoor map, in: 2014 International Conference on Indoor Positioning and Indoor Navigation (IPIN), 2014, pp. 646–655. doi:10.1109/IPIN.2014.7275539.